AEROBICALLY ENHANCED NANOBIOREMEDIATION OF DIESEL OIL CONTAMINATED SOIL AND WATER USING MYCOSYNTHESIZED SILVER NANOPARTICLE AS BIOSTIMULATING AGENT

Bright Obidinma Uba[*] and Genevieve Onyinye Obiefuna

Department of Microbiology, Chukwuemeka Odumegwu Ojukwu University, P.M.B.02 Uli, Anambra State, Nigeria

*Corresponding Author Email Address: bo.uba@coou.edu.ng   Phone: +2348069693773

ABSTRACT
To demonstrate the potential use of myco - synthesized silver nanoparticles in the nano -bioremediation of hydrocarbons contaminated soil and water using diesel oil as a model pollutant, a laboratory study with the objective of evaluating enhanced aerobic nano – bioremediation of diesel oil contaminated soil and water using was performed. The myco - synthesized silver nanoparticle was physico – chemically characterized using standard nanotechnological procedures. Soil and water samples were artificially contaminated with diesel oil and exposed to 5-, 10- and 15-mL concentrations of the myco - synthesized silver nanoparticle under ambient conditions for 60 days treatment periods. The results revealed that the physicochemical and spectral outcomes obtained confirmed the particle to be silver nanoparticle (AgNPs). The degradation of diesel oil residue after each treatment periods was evaluated spectrophotometrically. The result showed the ten and fifteen millilitre concentrations had the highest percentage degradative values of 93.40 % and 92.90 % after 60 days while the same concentrations had the lowest percentage degradative efficiency values 88.00 % and 84.90 % after day 1 in diesel oil contaminated water and soil, respectively. The exposure of AgNPs at different doses to waste diesel oil contaminated water and soil does not significantly ($P > 0.05$) quicken the nano - degradation of waste diesel oil. The reactions kinetics satisfactorily followed either first - order or second - order kinetics while the rate constant increases with a corresponding decrease in half -life time. Therefore, the study showed that myco - synthesized silver nanoparticle could be effective in the rehabilitation of diesel oil polluted environment.

Keywords: Integrated approach, Nanotechnology, Rehabilitation, Silver nanoparticle, Soil, Water.

INTRODUCTION
World-wide increase for fossil fuel has led to increase in petroleum exploration, refining and other associated industrial activities in developed and developing countries like Nigeria (Latinwo and Agarry, 2015). As a result of these activities, a substantial amount of water bodies and soil in Nigeria are exposed to severe contamination from hydrocarbons. This action had resulted into a negative consequence on the surrounding environment of the polluted area such as loss of terrestrial and aquatic life, decrease in yield of the contaminated site and threat to well-being of the living organisms inhabiting these sites (Ogujuofor *et al*., 2021).
Since the aquatic and terrestrial ecosystems are worsening day by day as a result of pollution, a promising technology must emerge to eliminate both public and human health threatening contaminants from it. Although there are a lot of physical, chemical and biological technologies applied for pollutant elimination, nano-bioremediation has become prominent as it is an integrated approach that applies both nanotechnology and bioremediation together to achieve a remediation that is more effectual, a lesser amount of time, cheaper and eco - friendly than the individual processes or several other technologies (Singh *et al*., 2020). Integrated approach could overwhelm the shortcomings of individual processes and can ultimately offer healthier remediation outcomes.

Fungal endophytes are reported to secrete diverse group of biomolecules extracellularly which are capable of reducing metal salts at rapid scale under optimized conditions (Azmath *et al*., 2016). One such endophyte *Colletotrichum* sp. ALF2-6 is isolated from healthy leaf of *Andrographis paniculata* and employed for rapid synthesis of silver nanoparticles (Azmath *et al*., 2016). The synthesized nanoparticles were evaluated for bactericidal activity against significant human pathogens (Azmath *et al*., 2016). Examples of fungi used for the synthesis of silver nanoparticles so far are *Verticillium* sp., *Phoma* sp., *Fusarium oxysporium, Fusarium semitectum, Fusarium solani, Trametes versicolor, Coriolus versicolor, Phanerochaete chrysosporium, Aspergillus fumigatus, Aspergillus flavus, Aspergillus clavatus, Aspergillus terreus, Saccharomyces cerevisiae* (Rajpu *et al*., 2017; Das *et al*., 2019; Elegbede and Lateef, 2019). Several researchers have evaluated bioremediation processes based on individual approaches with less examination of an integral technology like nano – bioremediation (Agarry *et al*., 2013; Agarry and Oghenejoboh, 2015; Agarry *et al*., 2015; Latinwo and Agarry, 2015; Kachieng'a and Momba, 2017). Also, most of the available literatures on nano -bioremediation focus on the pollutant degradation efficiencies with less attention on the degradative kinetics modelling and mechanisms of the technology and justify the present study. The present study tends to examine and evaluate the enhanced nano – remediation of diesel oil contaminated soil and water under aerobic conditions. The modelled kinetics of diesel oil nano – remediation process as well as assessment of the nano – remediation half-life time was also carried out.

MATERIALS AND METHODS
Collection of Specimen
Also, *Mannihot esculenta* (cassava) leaves were harvested using a sharp knife, placed in a sterile cylindrical plastic container and transported immediately to Microbiology Project Laboratory,

Chukwuemeka Odumegwu Ojukwu University, Uli, Campus, Anambra State, Nigeria.

Isolation of Fungal Endophyte
By adopting the modified method of Marchut-Mikolajczyk *et al*. (2010), the following surface sterilization conditions were applied: 70 % ethanol for 3 min, 1 % sodium hypochlorite for 12 min and 70 % ethanol for 30 sec. After the final ethanol step, the plant parts were rinsed five times with a sterile distilled water. Surface-sterile plant samples were cut with a sterile scalpel into the small pieces (~1 cm) under sterile conditions and placed on the sterile Potato Dextrose Agar media (PDA). The efficiency of the sterilization process was verified by pipetting 100 μL of water from the last wash onto PDB medium and monitoring possible microbial growth.

Identification of the Fungal Endophyte
The fungal morphology was studied macroscopically by observing the colony features (colour, shape, size and hyphae), and microscopically by a compound light microscope using lactophenol cotton blue stained slide mounted with a small portion of the mycelium (Alsohaili and Bani-Hassan, 2018).

Fungal Biomass Preparation
For fungal biomass preparation, the selected fungal culture was grown in the liquid medium containing (g/L): KH_2PO_4 7.0; K_2HPO_4 2.0; $MgSO_4.7H_2O$ 0.1; $(NH_4)_2SO_4$ 1.0; yeast extract 0.6 and glucose 10.0. Flask containing medium was incubated for 7 days at 28 ± 2 °C. After the incubation, the biomass was harvested through centrifugation at 4000 rpm for 25 min and washed with distilled water. Thereafter, the biomass was added to 100 mL of deionized water and further incubated for 72 h. After the incubation, the microbial filtrate was obtained by passing the suspension through Whatman No. 1 filter paper (Moustafa, 2017).

Silver Nitrate Solution Preparation
By adopting the method of Moustapha (2017), 5 mM silver nitrate ($AgNO_3$) solution was prepared and stored in amber coloured bottle.

Synthesis of the Silver Nanoparticle
In this study, the fungal filtrate was dispensed into burette followed by drop wise addition of the aqueous solutions of 5 mM $AgNO_3$ in 1:1 ratio and then heated at 70 °C on magnetic stirrer until the formation of silver nanoparticles with physical dark brown colour observation (Shittu and Ihebunna, 2017).

Characterization of the Synthesized Silver Nanoparticle
The methods of Fazlzadeh *et al.* (2016) and Moustafa (2017) were adopted in the characterization of the myco - synthesized silver nanoparticle. In this study, the reducing and capping agents were characterized using Fourier transform infra-red (FTIR) spectroscopy. The maximum surface plasmon resonance (SPR) was detected using UV-VIS spectrophotometric analysis at wavelength ranging from 200 – 1100 nm. The crystalline nature of the particle was determined using X-ray diffraction analysis and the crystallinity index (CI) was calculated. The morphological feature of the particle was determined using Scanning electron microscopic analysis.

Artificial Contamination of Water and Soil Sample
By adopting the method of the Ekundayo *et al*. (2020) the artificial contaminated soil was prepared by mixing 5 mL of diesel oil and 50 g of unpolluted garden soil in a 100 mL volumetric flask while the artificial contaminated water was prepared by mixing 5 mL of diesel oil and 40 mL of distilled water in same capacity volumetric flask above.

Nano - remediation Setup
In this method, 10 mL sterile basal medium, and 5-, 10- and 15-mL suspensions of the myco - synthesized silver nanoparticles were aseptically transferred into three volumetric flasks each containing 40 mL of sterile artificial contaminated water, respectively. Similarly, equal volume of the above-mentioned catalysts and basal medium were also aseptically transferred into three volumetric flasks containing 50 g of sterile artificial contaminated soil, respectively. The artificial contaminated water and soil without the catalysts served as controls. Each of the volumetric flasks were labelled appropriately and incubated under shaking condition at 37 °C for 60 days (Ekundayo *et al*., 2020). After incubation, N-hexane was used to extract the degraded residual oil, and the degraded residual diesel oil was determined spectrophotometrically at $OD_{540 nm}$ using N-hexane as blank at two weeks intervals. The experiment was done in replicates. Also, the percentage of the diesel oil biodegraded was then calculated using equation 1 (Kachieng and Momba, 2017) below:

Where Co is the initial oil weight and Cr is the residual oil weight.

Diesel Oil Degradation Kinetics
The rate oil degradation was described by pseudo first order and second order kinetics, and the values were calculated using equations 2 and 3 (Bhuiyan *et al*., 2020):

$$LnCo/C_t = k_1t \qquad (2)$$

$$1/C_t - 1/Co = k_2t \qquad (3)$$

where C_t is the weight of hydrocarbon (mg/kg) at a certain time, Co is the initial weight of hydrocarbon (mg/kg), *k* is the rate constant of the change in the oil weight (day^{-1}) and *t* is the incubation duration (day).
The time required for 25, 50 and 75 % oil degradation designated as T_{25}, T_{50} and T_{75} were determined from equations (4), (5) and (6).

$$T_{25} = \frac{0.288}{k} \qquad (4)$$

$$T_{50} = \frac{0.693}{k} \qquad (5)$$

$$T_{75} = \frac{1.386}{k} \qquad (6)$$

Where k is the rate constant of the oil degradation reaction.

Statistical Management
The data were subjected to descriptive statistics. The mean values subjected to one way analysis of variation (ANOVA) followed by Dunnet and Tukey`s multiple comparison test using GraphPad

Aerobically Enhanced Nanobioremediation of Diesel Oil Contaminated Soil and Water Using Mycosynthesized Silver Nanoparticle as Biostimulating Agent

76

Prism version 8.0.2. The obtained values less than 0.05 were considered significant at 95 % confidence intervals.

RESULTS AND DISCUSSION
Identity Profile
In this study, nanoparticles capable of degrading diesel oil were synthesized from fungal biomass of endophytic fungus. The result of the cultural and microscopic feature of the fungal isolate is clearly shown in Table 1. From the table, the endophytic mould isolate from the leave of *M. esculenta* showed a deep brown colony, with smooth wall and surface, rapid growth and reverse uncoloured. Microscopically, the spore is sporangiophore, long non - septate hollow hypha with sporangiospore borne in sporangium which was identified as *Aspergillus niger* using the most typical and distinctive keys in fungal proof of identity by comparing their colonial and microscopic features with those identified taxa (Klich, 2002; Samson and Varga, 2007). Endophytic *A. niger* has been isolated and documented by several workers (Jones *et al*., 2012; Flewelling *et al*., 2013;

Maadon *et al*., 2018; Hussein *et al.,* 2019). The synthesis of the silver nanoparticles was physically characterized by colour change from colourless to dark brown which typified silver nanoparticle formation. This colour change could be due to the activity of metabolites involved in the plant extract biomass filtrate (Rajput *et al*., 2017). Several endophytic moulds with silver nanoparticle synthesis potentials have been reported and documented (Azmath *et al*. 2016; Das *et al*. 2019; Rajpu *et al*. 2017). The extracellular synthesis of silver nanoparticles is more advantageous owing to the fact that it forms easy to downstream the nanoparticles compared to the intracellular synthesis. The obtained nanoparticles will be free from any bio-mass, toxic material and any solvent residues (Azmath *et al*. 2016).

**Table 1:** Cultural and microscopic feature of the fungal isolate

Isolate	Cultural character	Microscopic character	Identity
Fungal strain	Deep brown colony, downy textrure, smooth walled and surface, rapid growth, reverse uncoloured.	The spore is sporangiophore, the hyphae is hollow that, is, non - septate hypha with sporangiospore borne in - sporangium, the hyphae is longer.	*Aspergillus niger*

Characteristic Profile of the Biosynthesized Silver Nanoparticle (AgNPs)

Functional group profile
In order to confirm the AgNPs formation, further analyses were carried out on the silver nanoparticles to ascertain their physico - chemical characteristics. In this study, the result of the Fourier transform- infra red spectral peaks of the green synthesized nanoparticles are shown in Figure 1 A. From the figures, the peaks between 700 cm^{-1} and 900 cm^{-1} correspond to strong CH$_3$− metal groups due CH$_2$ rocking vibration. The peaks between 1000 cm^{-1} and 1160 cm^{-1} revealed there was strong C-O (carbohydrate group) stretching vibration. Peaks between 1180 cm^{-1} to 1470 cm^{-1} showed a strong B-O (haloboroxine group) stretching vibration. In peaks 1555 cm^{-1} to 1660 cm^{-1}, there was a strong C
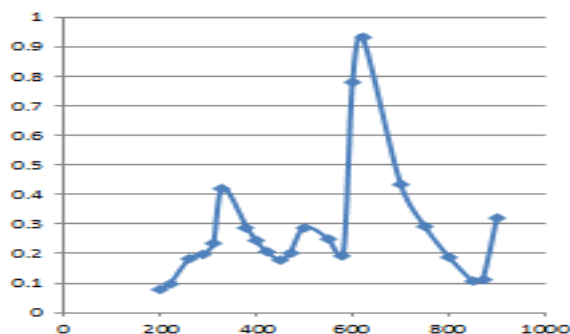
= N (pyroline) stretching vibration. From 1685 cm^{-1} to 1700 cm^{-1}, variably strong C = O (*α, β*- unsaturated ketones) stretching vibration. From 1930 cm^{-1} to 1955 cm^{-1}, there was a strong asymmetric C = C = C (allenes) stretching vibration. From 2130 cm^{-1} to 2300 cm^{-1}, showed a (diazonium salts) NN (triple bond) stretching vibration. Bands from 2370 cm^{-1} to 3300 cm^{-1}, showed a variable N$^+$-H (hydrogen bonded salts) stretching vibration. The peaks between 3330 cm^{-1} to 3550 cm^{-1}, showed weak asymmetric NH$_2$ stretching vibration. The peaks between 3551 cm^{-1} to 3800 cm^{-1}, showed medium O-H stretching vibration (cellulose group). The results in Figures 4.1 A - B revealed the major and minor peaks ranged from 700 cm^{-1} – 3,800 cm^{-1}. The presence of these different functional groups and metabolites such as carbohydrate, amine and cellulose groups in the samples known as capping agents help to form a coat covering on the silver nanoparticles that stabilizes the metallic nanoparticle and prevents cluster in the medium. Earlier FTIR analysis and profiling, revealed the role of biomolecules which reduce the silver nitrate and bind onto the nanoparticles and stabilize them hence preventing aggregation (Azmath *et al*., 2016)
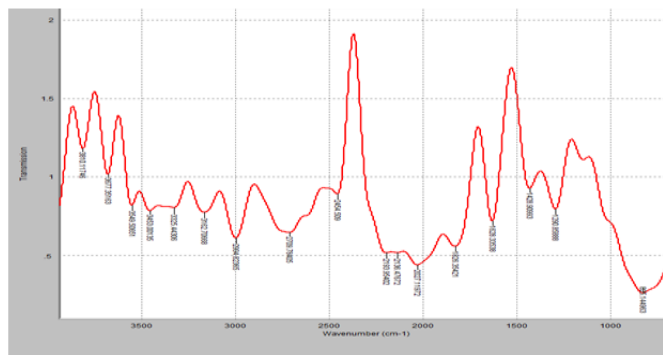
Figure 1: Spectral profile of *A. niger* synthesized silver nanoparticle

UV-VIS spectral profile
Figure 2 showed the UV-VIS spectroscopy absorbency peaks of *A. niger* synthesized AgNPs. From the result, the maximum peak of *A. niger* was 620 nm at 0.933 absorbance while the minimum peaks of *A. niger* was 200 nm at absorbance of 0.078, respectively. The myco-synthesized AgNPs showed the maximum peak of *Aspergillus niger* to be 620 nm which a very high surface plasmon resonance. This result contradicted the publication of Moustafa (2017) which reported that the sharp bands of silver nanoparticles synthesis by *Penicillium Citreonigum Dierck*. were observed around 400 – 450 nm and the reason could be due to species differences.

Aerobically Enhanced Nanobioremediation of Diesel Oil Contaminated Soil and Water Using Mycosynthesized Silver Nanoparticle as Biostimulating Agent

77

**Figure 2:** UV-VIS spectral of *A. niger* synthesized silver nanoparticle

Phase purity and crystalline structural profile
The result of the crystalline characteristics of the biosynthesized silver nanoparticle are presented in Table 2 and shown in Figure 3.
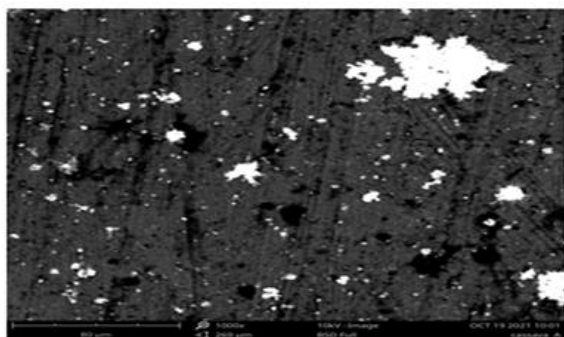
From the result, the XRD peaks of nanoparticles was clearly distinguishable and broad indicating an ultra - fine nature. From the Table 2 and Figure 3, the XRD spectrum of *A. niger* synthesized AgNPs showed characteristic intense peaks at 2Ɵ = 62.07 and 65.59 which corresponds to hkl (200 and 210, respectively) plane of face centered cubic silver. The crystal size of myco-synthesized AgNPs was obtained as 50 nm from the XRD pattern by the Debye-Scherrer equation. Anjana and Geetha (2019) reported that the average size of the AgNPs synthesized was approximately to be ~13 nm which is obtained using similar formula. Previous study by Rajput *et al.* (2017) reported four Bragg's peaks at 38.45, 45.75, 66.45 and 77.95 of silver nanoparticles synthesized from *Pestalotiopsis versicolor* and correspond to the cubic facets of the particles which justifies the standard diffraction pattern of silver nanoparticles and the result obtained was in agreement with the standard diffraction of earlier scientific reports.

Table 2: Phase purity and crystalline characteristic of the green synthesized silver nanoparticle

Synthesized AgNPs	Peak no.	2Ɵ	CosƟ	SinƟ	FWHM	β radian	Crystaline size 'D' nm	Hkl identified from peak
A. niger	1	62.07	0.8568	0.5156	0.9446	0.0165	9.81	200
	2	65.59	0.8406	0.5416	0.9446	0.0165	10.00	210

Key: AgNPs = Silver nanoparticles, Ɵ = Theta; FWHM = full width at half maximum; β = Beta; hkl = integers representing lattice planes.
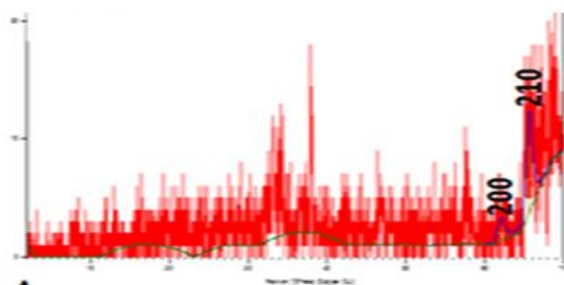
Figure 3: XRD pattern of *A. niger*
Key: XRD = X - ray diffraction; AgNPs = Silver nanoparticle

Figure 4: Scanning electron microscope image of the silver nanoparticle synthesized using *A. niger*

Diesel oil Degradation Profile
Silver nanoparticles (AgNPs) because of their environmental feasibility, ecologically sound behavior, and availability of large surface area for microbes, were known to remediate industrial wastewater. However, studies related to the use of AgNPs to remediate petroleum waste contaminated soils provide inconsistent findings (Sattar *et al.*, 2022). In this study, nano - catalyst synthesized from *A. niger* fungal biomass extract was used to test for their biodegradative abilities on waste diesel oil contaminated water and soil samples. The results of the time course for the biodegradation of the diesel oil contaminated water and soil under *A. niger* nanoparticle treatment are shown in Figures 5A – B. With slight changes in concentration of the water and soil controls in all the treatment regimens after 60 days, it was observed that the concentration of the diesel oil decreased in all treatments with increase in biodegradation time 1, 14, 28, 42 and 60 days with 10 mL having lowest values of 83.29, 59.28, 38.88, 32.08 and 19.68 mg/kg in diesel oil contaminated water and soil, respectively. The possible reason for the low residual hydrocarbon contents in the lower concentrations over the high concentrations of the silver nanoparticles treatments could be due to some sort of inhibitory effect of AgNPs nanoparticles on the natural hydrocarbon biodegraders. The results of the percentage efficiency of *A. niger* nanoparticle in biodegradation of diesel oil contaminated water and soil are shown in Figures 6A – B. There was slight change in the percentage degradative efficiency values of untreated water and soil (control) (87.40 – 87.76 %), respectively. Ten and fifteen millilitre concentrations had the highest percentage degradative

Aerobically Enhanced Nanobioremediation of Diesel Oil Contaminated Soil and Water Using Mycosynthesized Silver Nanoparticle as Biostimulating Agent

78

values of 93.40 % and 92.90 % after 60 days while the same concentrations had the lowest percentage degradative efficiency values 88.00 % and 84.90 % after day 1 in diesel oil contaminated water and soil, respectively. The present study showed that AgNPs application in single treatment regimen and at different concentration to waste diesel oil contaminated waters and soils does not significantly (P > 0.05) accelerate the degradation of waste diesel oil. The result of this study is in conformity with the

conclusion drawn by Sattar *et al.* (2022) and Beddow *et al.* (2014) who reported that AgNPs alone did not accelerate the degradation of TPHs and there was no noticeable increase in the bacterial population of the petroleum waste-contaminated soils.
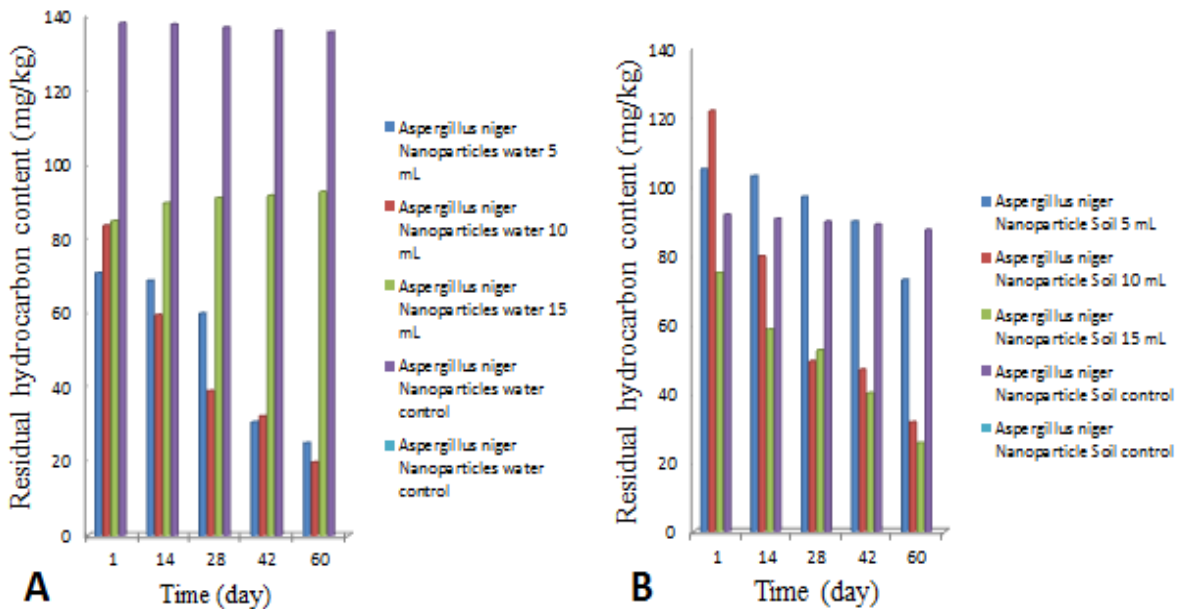
Figure 5: (A) Time course for the biodegradation of the diesel oil contaminated water under *A. niger* nanoparticle treatment. (B) Time course for the biodegradation of diesel oil contaminated water under *A. niger* nanoparticle treatment.
Key: mg/kg = Milligram per kilogram, mL = Milligram
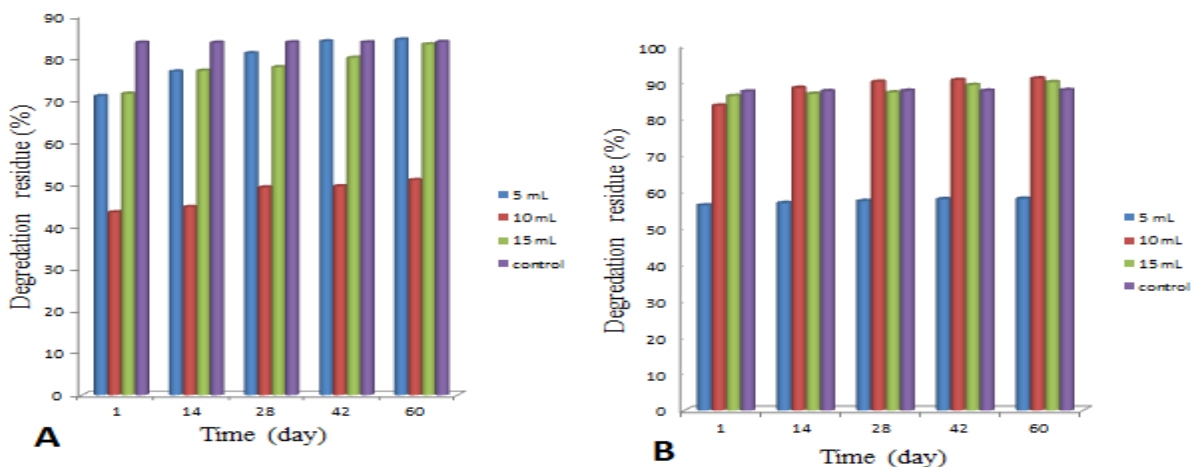
Figure 6: (A) Percentage efficiency of *A. niger* nanoparticle in biodegradation of diesel oil contaminated water. (B) Percentage efficiency of *A. niger* nanoparticle in biodegradation of diesel oil contaminated soil.
Key: mL =Mililitre, % = Percentage

Aerobically Enhanced Nanobioremediation of Diesel Oil Contaminated Soil and Water Using Mycosynthesized Silver Nanoparticle as Biostimulating Agent

79

Kinetic and Half -life Profile

Monitoring the process and progress of bioremediation is very crucial. The kinetics of biodegradation processes is solely dependent on the speed and development of the efficient removal of oil in any contaminated water bodies or normal environment (Kachieng's and Momba, 2017). In this study, a pseudo first-order and second order kinetic models were fitted to the biodegradation data as shown in Figures 7A – D to evaluate the biodegradation rate and to determine the corresponding T_{25}, T_{50} and T_{75} degradation times in the different remediation treatments as presented in Table 3 respectively. The Figures 7 showed the first order (A and C) and second order (B and D) linear kinetic plots of diesel oil contaminated water and soil biodegradation at different concentration of *A. niger* synthesized silver nanoparticle. The result revealed that *A. niger* nanoparticle treated water and soil at different concentrations including control were all fitted in second order rate constant (K_2) with R^2 values of 0.8871, 0.9871, 0.9834, 0.9777, 0.9008, 0.9097, 0.8852 and 0.9909, respectively. The results revealed that the degradation of waste diesel oil was both dose or concentration dependent and dose or concentration independent as the reaction times proceed; both the first order and second order kinetics satisfactorily described (R^2 values between 0.8094 to 0.9909) the biodegradation of the diesel oil-based contaminants under abiotic conditions. The biological half-life is the time taken for a substance to lose half of its amount. Biodegradation half-lives are needed for many applications such as chemical screening, environmental fate modeling and describing the transformation of pollutants (Agarry and Oghenejoboh, 2015).

The Table 3 showed the results of the comparison for degradation kinetics of diesel oil contaminated soil and water by *A. niger* for 60 days. From the Table 3 result, the waste diesel oil degradation reached its half-life by 9.493 day^{-1} for 5 mL dose while it took only 8.772 day^{-1}, 12.158 day^{-1} and 23.897 day^{-1} for 10 mL, 15 mL and control of the water nanoparticle treated doses correspondingly. Also, the waste oil degradation reached it half – life by 19.25 day^{-1} for 5 mL dose while it took only 16.116 day^{-1}, 15.75 day^{-1} and 19.800 day^{-1} for 10 mL, 15 mL and control of the soil nanoparticle treated doses, respectively. From the result, it is to be noted that the higher the biodegradation rate constants, the higher or faster is the rate of biodegradation and consequently the lower is the half-life time. Although there was increase in the amount of waste diesel oil lose as the degradation time (T_{25}, T_{50} and T_{75}) increases, the 5 mL concentration of the nanoparticles had the lowest T_{50s} in all the treatment regimens revealing that 5 mL nanoparticle concentration removes waste diesel oil faster than 10 mL and 15 mL, respectively. Therefore, the value of the kinetic parameter in order of their degree of efficiencies of the treatment regimens in the cleanup of water and soil polluted with waste diesel oil is in the following descending order: 5 mL > 10 mL > 15 mL > control (untreated) water or soil while treated water > treated soil, respectively. The findings of this study corroborated with the published bioremediation reports of several authors who had similar trends in their studies (Agarry *et al*. 2013; Agarry and Oghenejoboh, 2015; Agarry *et al*. 2015; Latinwo and Agarry, 2015; Kachieng's and Momba, 2017).
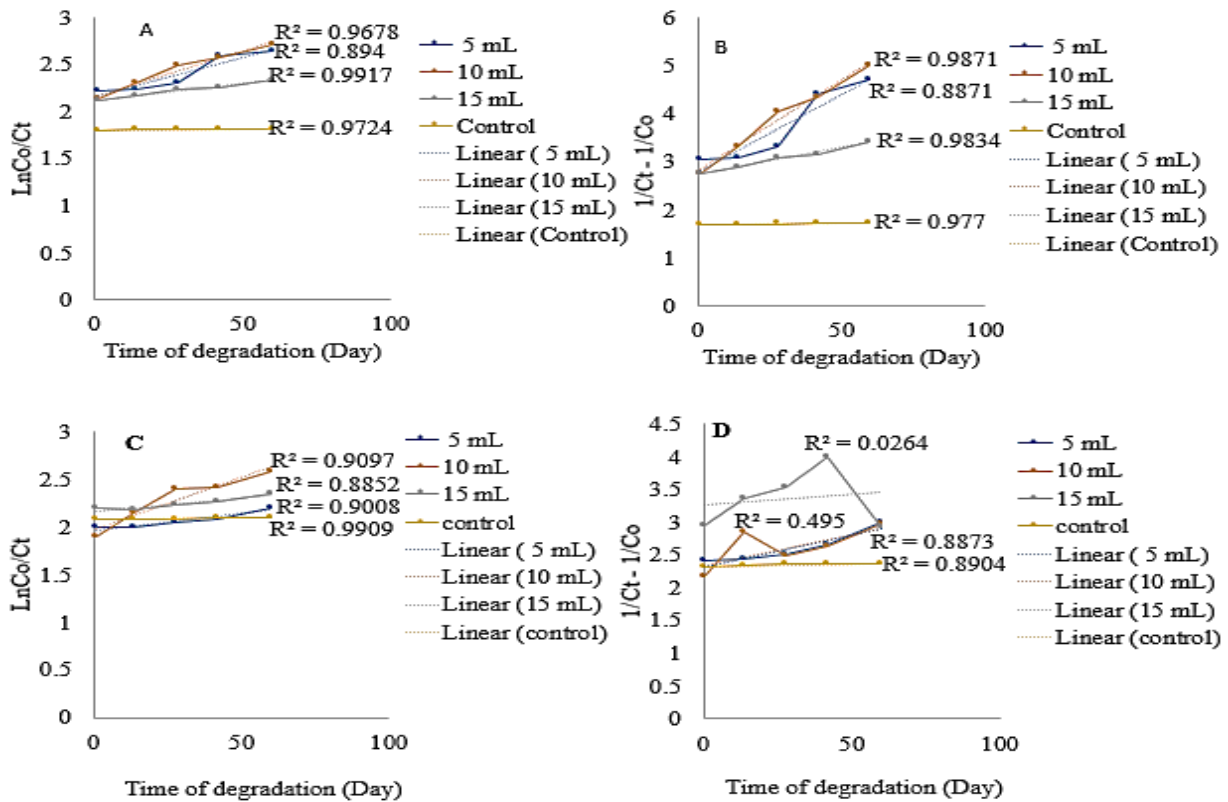
Figure 7: First order (A and C) and second order (B and D) linear kinetic plot of diesel oil contaminated water and soil biodegradation at different concentration of *A. niger* synthesized silver nanoparticle

Table 3: Comparison for degradation kinetics of diesel oil by *A. niger* nanoparticle for 60 days

Sample type	Treatment concentration (mL)	Kinetic parameter	Waste diesel oil
Diesel oil contaminated water	5	Second order rate constant (k_2) (day^{-1})	0.073
		T_{25}	3.945
		T_{50}	9.493
		T_{75}	18.986
	10	Second order rate constant (k_2) (day^{-1})	0.079
		T_{25}	3.646
		T_{50}	8.772
		T_{75}	17.544
	15	Second order rate constant (k_2) (day^{-1})	0.057
		T_{25}	5.053
		T_{50}	12.158
		T_{75}	24.316
	control	Second order rate constant (k_2) (day^{-1})	0.029
		T_{25}	9.931
		T_{50}	23.897
		T_{75}	47.793
Diesel oil contaminated soil	5	First order rate constant (k_1) (day^{-1})	0.036
		T_{25}	8.000
		T_{50}	19.250
		T_{75}	38.500
	10	First order rate constant (k_1) (day^{-1})	0.043
		T_{25}	6.698
		T_{50}	16.116
		T_{75}	32.233
	15	First order rate constant (k_1) (day^{-1})	0.044
		T_{25}	6.545
		T_{50}	15.750
		T_{75}	31.500
	control	First order rate constant (k_1) (day^{-1})	0.035
		T_{25}	8.229
		T_{50}	19.800
		T_{75}	39.600

Conclusion

Generally, the study revealed that the potential of biomass filtrate of *A. niger* in the green synthesis of silver nanoparticle. The synthesized $AgNO_3$ nanoparticles demonstrated bioremediation effectiveness against diesel oil contaminated water and soil. The effectiveness of the bioremediation is in the following descending order: 5 mL > 10 mL > 15 mL > control (untreated) water or soil while treated water > treated soil, respectively. The study has help to consolidate the data on the efficiency of nanoparticles in the biodegradation of hydrocarbon contaminated water and soil ecosystems. Future study should explore the potentials of these nano - catalysts in the nano - biodegradation of other hydrocarbons aside diesel oil as well as undertake the potentials of other types of nanoparticles in the bioremediation of waste diesel oil contaminated ecosystems.

Aerobically Enhanced Nanobioremediation of Diesel Oil Contaminated Soil and Water Using Mycosynthesized Silver Nanoparticle as Biostimulating Agent

81

REFERENCES

Agarry, S. E., Aremu, M. O. and Aworanti, O. A. (2013). Kinetic modelling and half- life study on bioremediation of soil co-contaminated with lubricating motor oil and lead using different bioremediation strategies, soil and sediment contamination. *An International Journal*, *22*(7): 800 - 816.

Agarry, S. E. and Oghenejoboh, K. M. (2015). Enhanced aerobic biodegradation of naphthalene in soil: kinetic modelling and half-life study. *International Journal of Environmental Bioremediation and Biodegradation*, *3* (2): 48 – 53.

Agarry, S. E., Oghenejoboh, K. M. and Solomon**,** B.O. (2015). Kinetic modelling and half-life study of adsorptive bioremediation of soil artificially contaminated with bonny light crude oil. *Journal of Ecological Engineering*, *16* (3): 1 – 13.

Alsohaili, A. S. and Bani-Hasan, M. B. (2018). Morphological and molecular identification of fungi isolated from different environmental sources in the northern eastern desert of Jordan. *Jordan Journal of Biological Sciences, 11(3)*: 329 – 337

Anjana, R. and Geetha, N. (2019). Degradation of methylene blue using silver nanoparticles synthesized from *Cynodon dactylon* (L.) Pers. leaf aqueous extract. *International Journal of Scientific and Technology Research, 8* (9): 225 – 229.

Azmath, P., Baker, S., Rakshith, D. and Satish, S. (2016). Myco - synthesis of silver nanoparticles bearing antibacterial activity. *Saudi Pharmaceutical Journal*, 25 (1): 140 – 146.

Beddow, J., Stölpe, B., Cole, P.A., Lead, J.R., Sapp, M., Lyons, B.P., McKew, B., Steinke, M., Benyahia, F. and Colbeck, I. (2014). Estuarine sediment hydrocarbon-degrading microbial communities demonstrate resilience to nanosilver. *International Biodeterioration and Biodegradation*, *96*: 206 – 215.

Bhuiyan, M.S.H., Miah, M.Y., Paul, S.C., Aka, T.D., Saha, O., Rahaman, M.M., Sharif, M.J.I., Habiba, O., Ashaduzzaman, M. (2020). Green synthesis of iron oxide nanoparticle using *Carica papaya* leaf extract: application for photocatalytic degradation of remazol yellow RR dye and antibacterial activity. *Heliyon*, : e04603

Das, A., Kamle, M., Bharti, A. and Kumar, P. (2019). Nanotechnology and it's applications in environmental remediation: an overview. *Vegetos*, https://doi.org/10.1007/s42535-019-00040-5

Ekundayo, F. O., Orisadipe, D. B. and Onifade, I. A. (2020). Degradative ability of silver particles synthesized by gram-negative bacteria of some crop's rhizosphere on crude oil polluted soil. *Asian Plant Research Journal, 4* (4): 25 – 33.

Elegbede, J.A., & Lateef, A. (2019). Green nanotechnology in Nigeria: The research landscape, challenges and prospects. *Annals of Science and Technology, 4* (2): 6 – 38.

Fazlzadeh, M., Rahmani, K., Zarei, A., Abdoallahzadeh, H., Nasiri, F. & Khosravi, R. (2016). A novel green synthesis of zero valent iron nanoparticles (NZVI) using three plant extracts and their efficient application for removal of Cr (VI) from aqueous solutions. *Advanced Powder Technology,* Article in Press: http://dx.doi.org/10.1016/j.apt.2016.09.003.

Flewelling, A.J., Johnson, J.A. and Gray, C.A. (2013). Isolation and bioassay screening of fungal endophytes from north atlantic marine macroalgae. *Bot. Mar. 56:* 287–297. Jones, E.B.G., Pang, K.L. and Stanley, S.J. (2012). *Fungi from Marine Algae. In Marine Fungi and Fungal-Like Organisms*. Jones, E.B.G. and Pang, K.-L. (Eds.). Berlin, Germany: Walterde Gruyter.

Hussein, Z.A., Ghfil, A. and Mohammed, D.Y. (2019). Isolation and identification of some endophytic fungi from some local algae *Plant Archives 19 (1):* 1410 – 1418.

Kachieng'a, L. and Momba, M.N.B. (2017). Kinetics of petroleum oil biodegradation by a consortium of three protozoan isolates (*Aspidisca* sp., *Trachelophyllum* sp. and *Peranema* sp.). *Biotechnology Reports*, *15*: 125 – 131.

Klich, M.A. (2002). *Identification of Common Aspergillus species*. Utrecht, Netherlands: CBS Fungal Biodiversity Centre.

Latinwo, G. K. and Agarry, S. E. (2015). Kinetic modelling of bioremediation of water contaminated with bonny light crude oil using biostimulation-bioaugmentation agent. *Universal Journal of Environmental Research and Technology*, *5 (4):* 188 – 200.

Maadon, S.N., Wakid, S.A., Zainudin, I.I., Rusli, L.S., Mohdzan, M.S., Hasan, N.A., Shah, N.A.A. and Rohani, E.R. (2018). Isolation and identification of endophytic fungi from UiTMReserve Forest, Negeri Sembilan. *Sains Malaysiana, 47 (12):* 3025–3030. http://dx.doi.org/10.17576/jsm-2018-4712-1.

Marchut-Mikolajczyk, O., Piotr, D., Dominika, P. and Tadeusz, A. (2018). Biosurfactant production and hydrocarbon activity of endophytic bacteria isolated from *Chelidonium majus* L. *Microbial Cell Factories, 17*:171.

Moustapha, M. T. (2017). Removal of pathogenic bacterial from wastewater using silver nanoparticles synthesized by two fungal species. *Water Science, 31:* 164 − 176

Ogujoifor, I. F., Machido, D. A. and Atta, H. I. (2021). Effect of the application of goat dung on the bioremediation of polluted soil by hydrocarbon degrading bacteria: A microcosm study. *FUDMA Journal of Sciences 5 (1)*: 278 – 287.

Rajput, K., Agrawal, S., Sharma, J. and Agrawal, P. (2017). Myco - synthesis of silver nanoparticles using endophytic fungus and investigation of its antibacterial and azo dye degradation efficacy *Pestalotiopsis versicolor. KAVAKA, 49*:65 – 71.

Salunke, B.K., Sawant, S.S., Kang, T.K., Seo, D.Y., Cha, Y., Moon, S.A., Alkotaini, B., Sathiyamoorthi, E. and Kim, B.S. (2015). Potential of biosynthesized silver nanoparticles as nanocatalyst for enhanced degradation of cellulose by cellulase. *Journal of Nanomaterials*, *289410*:1 – 8.

Samson, R.A. and Varga, J. (2007). *Aspergillus* systematics in the genomic era. Utrecht Netherlands: CBS Fungal Biodiversity Centre.

Sarsar, V., Selwal, M.K. and Selwal, K.K. (2015). Biofabrication, characterization and antibacterial efficacy of extracellular silver nanoparticles using novel fungal strain of *Penicillium atramentosum* KM. *Journal of Saudi Chemical Society*, *19 (6):* 682 – 688.

Sattar, S., Siddiqui, S., Shahzad, A., Bano, A., Naeem, M., Hussain, R., Khan, N., Jan, B.L. and Yasmin, H. (2022). Comparative analysis of microbial consortiums and nanoparticles for rehabilitating petroleum waste contaminated soils. *Molecules, 27:* 1945.

Singh, R., Behera, M. and Kumar, S. (2020). *Nano-Bioremediation: An Innovative Remediation Technology for Treatment and Management of Contaminated Sites*. In: R. N. Bharagava, and G. Saxena (Eds.), *Bioremediation of Industrial Waste for Environmental Safety* (pp. 165 – 182). Singapore: Springer Nature Pte Ltd. https://doi.org/10.1007/978-981-13-3426-9_7.

Aerobically Enhanced Nanobioremediation of Diesel Oil Contaminated Soil and
Water Using Mycosynthesized Silver Nanoparticle as Biostimulating Agent

82